Contribution from AT&T Bell Laboratories, Murray Hill, New Jersey 07974, and Chemistry Department, Brookhaven National Laboratory, Upton, New York 11973

Hydridic Atom Arrangement and Bonding in the Molecular Structure of $(C_2H_5)_4N^+[Re_2(\mu\text{-}H)_3H_6\{CH_3C(CH_2P(C_6H_5)_2)_3\}]^-\cdot CH_3CN$: A Complex Containing 10-Coordinated Rhenium

S. C. Abrahams,*† A. P. Ginsberg,*†‡ T. F. Koetzle,*§ P. Marsh,† and C. R. Sprinkle†

Received July 24, 1984

A complex obtained from the reaction of ReH_9^{2-} with triphos ($CH_3C(CH_2P(C_6H_5)_2)_3$) is found to be a nonahydride dimer in which ReH_9^{2-} is coordinated to Re(triphos)$^+$ via three H atoms and a Re–Re bond. The 10-coordinated Re atom in this compound, $(C_2H_5)_4N^+[Re_2(\mu\text{-}H)_3H_6\{CH_3C(CH_2P(C_6H_5)_2)_3\}]^-\cdot CH_3CN$, is the first example of a transition-metal atom with coordination number greater than 9, in a molecular compound. The structure of the compound was determined at 295 K by X-ray diffraction and at 80 K by neutron diffraction; it crystallizes in space group $P\bar{1}$ with $Z = 2$, $a = 12.384$ (3) Å, $b = 11.582$ (3) Å, $c = 19.323$ (4) Å, $\alpha = 101.89$ (2)°, $\beta = 94.80$ (2)°, and $\gamma = 109.53$ (2)° at 295 K and $a = 12.424$ (15) Å, $b = 11.553$ (5) Å, $c = 18.627$ (10) Å, $\alpha = 102.45$ (3)°, $\beta = 94.64$ (3)°, and $\gamma = 107.82$ (4)° at 80 K. Final X-ray diffraction agreement indicators on F_m are $R = 0.0226$, $R_w = 0.0262$, and $S = 1.594$ for 2565 independent observed reflections with $F_m > 3\sigma(F_m)$ and $R_{int} = 0.0122$; corresponding neutron indicators are $R = 0.1336$, $R_w = 0.0516$, and $S = 1.842$ for 2562 observations with $F_m^2 > 1.5\sigma(F_m)^2$ and $R_{int} = 0.083$. The Re–Re bond of 2.594 (1) Å passes obliquely through a face of the systematically distorted, equatorially girded ReH_9 trigonal prism (a 14-deltahedron). The other Re atom is octahedrally coordinated by the three bridging H and the three P atoms. The average bridging Re–H distance at 80 K is 1.86 (4) Å, the average terminal Re–H distance is 1.66 (6) Å, and the average Re–P distance at 295 K is 2.289 (4) Å. An SCF–Xα–SW calculation on $[Re_2(\mu\text{-}H)_3H_6(PH_3)_3]^-$ shows the Re–Re bond to be a $\sigma^2\pi^4$ triple bond. The Re–Re bonding orbitals also function as Re–H_{br} bonding orbitals; their dual bonding character permits the Re atom to achieve a coordination number greater than 9. In the visible region, $[Re_2H_9(triphos)]^-$ has absorption maxima at ~360 (ϵ 7.4 × 10^3) and ~335 (ϵ 7.4 × 10^3) nm. Xα-transition-state calculations assign this absorption to charge transfer from the phosphine-coordinated to the H_9-coordinated Re atom.

Introduction

Transition-metal polyhydride complexes form an extensive and diverse class of compounds. The metal coordination in nearly all known polyhydride complexes includes one or more non-hydride ligands, usually a high-field ligand such as a tertiary phosphine, which stabilizes the M–H bond. The only exceptions are the binary hydride complexes ReH_9^{2-}, TcH_9^{2-}, and FeH_6^{4-}. A preliminary communication[1] reported that the dinuclear heptahydride anion $[Re_2(\mu\text{-}H)_3H_4(triphos)]^-$ (triphos = $CH_3C(CH_2P(C_6H_5)_2)_3$), obtained from the reaction of ReH_9^{2-} with triphos, is the first example of a polyhydride complex in which the only non-hydride ligand is a metal atom bound by a triple bond. Further work has shown that, although this claim is correct, the complex contains two other hydride ligands in addition to those reported and it must be formulated as the dinuclear nonahydride anion $[Re_2(\mu\text{-}H)_3H_6(triphos)]^-$. Six terminal and three bridging H atoms in this anion form a distorted tricapped trigonal prism (a 14-deltahedron), similar to the arrangement in ReH_9^{2-}, about one of the Re atoms. The second Re atom caps a deltahedron face and is linked to the first Re atom by three hydrogen bridges and a metal–metal triple bond that passes through a quadrilateral face of the trigonal prism, with which it makes an angle of 44°. The triphos group is coordinated only to the second Re atom. Effectively, ReH_9^{2-} serves as a tetradentate ligand for Re(triphos)$^+$. Both 10- and 7-coordinated Re atoms are therefore present in the nonahydride dimer; this is the first observation of a coordination number greater than 9 for a transition-metal atom in a molecular compound.[2] In this paper we present the structural determination of the dirhenium nonahydride complex by X-ray diffraction at 295 K and by neutron diffraction at 80 K, together with an Xα–SW study on the model complex $[Re_2(\mu\text{-}H)_3H_6(PH_3)_3]^-$, which defines the metal–metal bond order and accounts for the bonding to the unusual 10-coordinated Re atom. We also report the results of new measurements of the ^{1}H NMR spectrum, as well as the infrared and optical spectra, of the complex. On the basis of Xα-transition-state calculations, the visible region absorption spectrum is assigned to charge transfer from the phosphine-coordinated to the H_9-coordinated rhenium atom.

Experimental Section

Preparation, Characterization, and Crystal Growth. All manipulations were conducted under argon or helium; solvents were distilled under nitrogen. The complex was prepared as described previously[1] and crystallized from MeCN–Et_2O to give the deep reddish orange[3] crystalline air-sensitive product. Anal. Calcd for $(C_2H_5)_4N[Re_2H_9\{CH_3C(CH_2P(C_6H_5)_2)_3\}]\cdot CH_3CN$: C, 52.02; H, 6.08; N, 2.38; P, 7.89. Found: C, 51.99; H, 6.17; N, 2.34; P, 7.91. Infrared spectra of Nujol and Fluorolube mulls of the complex at ambient temperature and at 80 K were measured with a Perkin-Elmer 683 spectrometer. ^{1}H NMR spectra were measured at 200 MHz with a Varian XL 200 spectrometer. Samples were dissolved in CD_3CN for measurements at 294 K and in C_2D_5OD for low-temperature measurements. Optical spectra of the complex in CH_3CN solution were measured at room temperature over the range 210–800 nm with a Cary Model 14R spectrophotometer. For the X-ray structure determination, crystals of $Et_4N[Re_2H_9(triphos)]\cdot MeCN$ were grown from a refrigerated saturated solution of the complex in 4:1 Et_2O–MeCN over a period of 24 h. Larger crystals for the neutron study were grown by the following procedure: 30 mg of the complex was dissolved in 5 mL of MeCN contained in a 25-mL centrifuge tube. The tube was closed by a cap through which an 0.5-mm hole had been bored; it was then enclosed in a flask containing 100 mL of Et_2O. After the solution stood for 25 days at 297 ± 1 K, the crystals were collected and washed with ether; the largest (1 × 1.1 × 1.5 mm) was marginally acceptable for the neutron diffraction measurements. Repeated attempts to grow larger, higher quality crystals were unsuccessful.

X-ray Diffraction. A sphere was ground from a prismatic crystal, mounted with arbitrary orientation on a Pyrex capillary, and epoxy-coated. Experimental and crystal variables are given in Table I.[4,5] Intensities of seven standard reflections were measured at 6-h intervals: all suffered a common linear decline with time, as given by $I_t = I_0(1 - 0.000519t)$ for t in hours. The maximum exposure was about 332 h, for

† AT&T Bell Laboratories.
‡ Present address: P.O. Box 986, New Providence, NJ 07974.
§ Brookhaven National Laboratory.

(1) Ginsberg, A. P.; Abrahams, S. C.; Marsh, P.; Ataka, K.; Sprinkle, C. R. *J. Chem. Soc., Chem. Commun.* **1984**, 1321.
(2) (a) Ligand coordination numbers greater than 9 are known for lanthanide and actinide metal complexes. These compounds nearly all involve bidentate ligands; the only example of 10-coordination by monodentate ligands of which we are aware is the recently reported compound $(NH_4)_4UF_{10}$.[2b] (b) Druzina, B.; Milicev, S.; Slivnik, J. *J. Chem. Soc., Chem. Commun.* **1984**, 363.
(3) ISCC-NBS Centroid Color Charts: *Natl. Bur. Stand. Circ.* (*U.S.*) **1964**, *No. 553* (supplement).
(4) Weber, K. *Acta Crystallogr., Sect. B: Struct. Crystallogr. Cryst. Chem.* **1969**, *B25*, 1174.
(5) *CAD-4 Operations Manual*; Enraf-Nonius: Delft, The Netherlands, 1982.

0020-1669/86/1325-2500$01.50/0

Table I. Experimental and Crystal Data for $Et_4N^+[Re_2H_9\{MeC(CH_2PPh_2)_3\}]^-\cdot MeCN$[a]

formula	$(C_8H_{20}N)^+[Re_2H_9\{CH_3C(CH_2P(C_6H_5)_2)_3\}]^-\cdot C_2H_3N$, $C_{51}H_{71}N_2P_3Re_2$
fw	1177.47
space group	$P\bar{1}$
a, Å	12.384 (3) [12.424 (15)]
b, Å	11.582 (3) [11.553 (5)]
c, Å	19.323 (4) [18.627 (10)]
α, deg	101.89 (2) [102.45 (3)]
β, deg	94.80 (2) [94.64 (3)]
γ, deg	109.53 (2) [107.82 (4)]
V, Å^3	2520.8 [2454.3]
no. of reflecns for cell params	25 [30]
range in 2θ, deg	18.2–32.4 [31–51]
temp, K	295 [80.0 (5)]
Z	2
d_{measd}, g cm^{-3} (298 K)	1.47 (5)
d_{calcd}, g cm^{-3}	1.551 [1.591]
μ, mm^{-1}	4.99[b] [0.2485]
cryst radius (dimens), mm	0.081 (4) [1 × 1.1 × 1.5]
μR	0.404
transmission factor range, %	54.9–55.2 [70.1–81.2]
F(000), e	1168
radiation	Mo Kα (λ = 0.71073 Å), graphite monochromator [λ = 1.15875 (12) Å, based on KBr a_0 = 6.6000 Å at 295 K, Ge(220) monochromator]
rlp scan:[c] angle, deg	2θ–ω: 0.85 + 0.35 tan θ [ω: $\Delta\omega$ = 4.2, step size 0.06]
rl range[c]	$-12 \leq h \leq 12$, $-11 \leq k \leq 11$, $-18 \leq l \leq 18$ [$-11 \leq h < 11$, $0 \leq k \leq 9$, $-17 \leq l \leq 17$]
max (sin θ)/λ, Å^{-1}	0.42 [0.495]
diffractometer	CAD-4 [4-circle at BNL HFBR]
control minicomputer[d]	PDP 11/40-8e [PDP 11/40]
max time/rlp, s	240 [280]
total no. of F_m	6376 [5061]
no. of Friedel pairs	3190 [295]
no. of indep $F_m > 3\sigma F_m$ [$F_m^2 > 1.5\sigma F_m^2$][e]	2565 [2562]
R_{int}[f]	0.0122 [0.049]

[a] X-ray diffraction values at 295 K are followed in brackets by the neutron diffraction values at 80 K. [b] See ref 4. [c] Abbreviations: rlp, reciprocal lattice point: rl, reciprocal lattice. [d] See ref 5 for software: for BNL software, see ref 39. [e] Remaining F_m not used in subsequent analysis. [f] $R_{int} = \sum(|F_m - \langle F_m\rangle|)/\sum F_m$.

a maximum correction of 17.2% in integrated intensity. The largest internal agreement factor for a standard reflection after correction for decline was 2.7%; the smallest, 1.4%. All integrated intensity measurements were corrected for Lorentz, polarization, absorption, and linear decline effects. The accuracy indicated by R_{int} in Table I suggested that the hydrogen atom scattering component could ultimately be recovered from the F_m quantities. The variance in F_m^2 was taken (cf. ref 6) as the larger of V_1 or V_2, where V_1 is the internal variance given by the difference between $F^2(hkl)$ and $F^2(\bar{h}\bar{k}\bar{l})$ and V_2 is the external variance as given by the sum of variances due to counting statistics, deviations from sample sphericity, and instrumental and scattering effects. In the final refinement cycles, F(100) was omitted. The magnitudes of 3190 F_m and σF_m values, including F(100), are deposited together with the final F_c values on the least-squares-derived absolute scale as supplementary material. No evidence for extinction was detected in the F_m data.

Neutron Diffraction. A prism bounded by {310}, {010}, and {001} faces, with volume about 1.61 mm^3, was mounted within an inert-atmosphere box in arbitrary orientation on a hollow aluminum pin and immediately placed in an indium-sealed can under nitrogen before being attached to the cold finger of an Air Products and Chemicals Inc. Model CS-202 Displex closed-cycle refrigerator. Neutron diffraction measurements

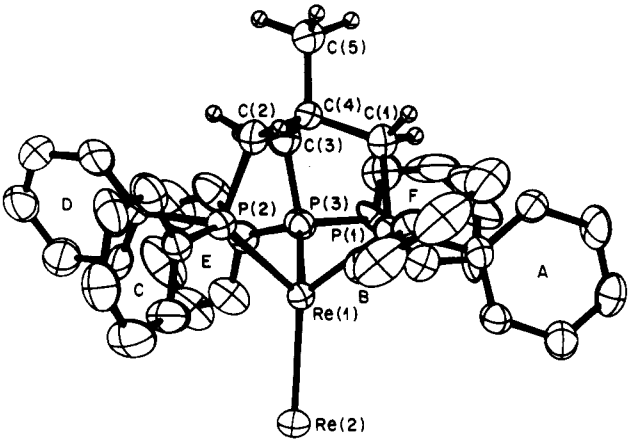

Figure 1. Perspective view of the anion at 295 K, with atom labeling and 35% probability thermal vibration ellipsoids, excluding the nine H atoms bonded to Re(2).

were made at the Brookhaven National Laboratory High-Flux Beam Reactor (see Table I) with the temperature held at 80 ± 0.5 K. The high mosaic spread led to the integrated intensity measurements being made by means of ω-step scans. A hemisphere of reciprocal space was measured, with three intensity standards ($\bar{3}38$, $\bar{4}45$, and $\bar{1}04$) determined every 100 reflections (or about every 10 h), to give a total of 5061 intensities including 152 standards and 13 measurements of an azimuthal scan performed on ($15\bar{1}$) near χ = 90°. This azimuthal scan provided a check on the absorption correction and also revealed some crystal splitting. Systematic variation in the standard intensities was not detected during the experiment. The scan profiles were integrated, the background being taken from seven steps at either end of the scan. Absorption corrections were made by the Gaussian numerical integration procedure.[7] Friedel pairs and multiple observations of the same reflections were averaged to yield 2562 independent values of $F_m^2 > 1.5\,\sigma_{cs}F_m^2$, with $R_{int}(F^2)$ = 0.083. Intensity variances were estimated from Poisson counting statistics. The variance from equivalent and replication measurements was invariably less than that given by counting statistics. The magnitudes of the 2562 F_m^2 and σF_m^2 values, together with the final F_c values on the absolute scale, are deposited as supplementary material.

The Laue symmetry of the crystal is $\bar{1}$, with no systematic absences. The high absorption of 1.06-μm light from a laser source, followed by rapid decomposition, precluded satisfactory testing for inversion centers by second-harmonic generation.[8] Neither a piezoelectric nor a pyroelectric signal was detected. The subsequent analysis confirmed the choice of space group as $P\bar{1}$.

Structure Solution and Refinement. The structure was derived by solving the Patterson function, based on X-ray diffraction structure amplitudes. Difference Fourier series followed by least-squares refinement on F_m^2 led rapidly to the location of all non-hydrogen atoms in the anion and eventually to those in the cation and in the solvate molecule. Atomic scattering factors used were for neutral atoms, including f' and f''.[9] Seven of the nine H atoms bonded to Re(2) and the six methylene H atoms in the $CH_3C(CH_2P(C_6H_5)_2)_3$ group (see C(1), C(2), and C(3) in Figure 1) were located from difference Fourier series and were varied in least-squares refinement without constraint in position or isotropic temperature factor magnitudes, with use of a locally modified version of ORFLS.[10] The two remaining H atoms, discovered only later as H(8) and H(9) in the neutron diffraction analysis, were finally identified with two of six residual electron density maxima with peak heights slightly less than 0.3 e Å^{-3}: only these two refined normally in subsequent least-squares analysis on including their associated eight additional positional and thermal parameters. It may be noted that the refinement behavior of the H atom parameters was partially correlated with the model used for the solvate molecule. The four electron-density maxima associated with the disordered solvate molecule at 295 K were each assigned an atomic occupancy of 0.75 and each position was thereafter refined with anisotropic temperature factors and C atomic scattering factors (see N, C(S) in Table II). The three H atoms in the solvate methyl group were omitted from all further calculations. The remaining 111 atoms in the

(6) Abrahams, S. C.; Bernstein, J. L.; Keve, E. T. *J. Appl. Crystallogr.* **1971**, *4*, 284.

(7) Busing, W. R.; Levy, H. A. *Acta Crystallogr.* **1957**, *10*, 180.
(8) Abrahams, S. C. *J. Appl. Crystallogr.* **1972**, *5*, 143.
(9) *International Tables for X-ray Crystallography*; Ibers, J. A., Hamilton, W. C., Eds.; Kynoch: Birmingham, England, 1974; Vol. IV.
(10) Busing, W. R.; Martin, K. O.; Levy, H. A. *J. Appl. Crystallogr.* **1973**, *6*, 309.

Table II. Final Atomic Coordinates (×10⁵ for Re, ×10⁴ for P, C, and N, and ×10³ for H) and Rms Thermal Displacements (×10² Å) at 295 K, by X-ray Diffraction

atom	*x*	*y*	*z*	*U*[a]	atom	*x*	*y*	*z*	*U*[a]
Re(1)	25358 (3)	86003 (4)	74266 (2)	22 (3)	C(3E)	5550 (14)	8254 (16)	9251 (8)	34 (9)
Re(2)	22831 (4)	101513 (4)	85224 (2)	27 (6)	C(4E)	6046 (13)	7359 (22)	9174 (10)	35 (17)
H(1)	300 (6)	1138 (7)	892 (4)	27 (4)	C(5E)	5954 (13)	6600 (17)	8493 (12)	35 (14)
H(2)	158 (7)	1103 (8)	823 (4)	30 (5)	C(6E)	5385 (12)	6805 (14)	7921 (7)	31 (8)
H(3)	138 (5)	914 (5)	765 (3)	21 (5)	C(1F)	5422 (9)	9241 (13)	7031 (5)	25 (9)
H(4)	241 (5)	845 (6)	832 (3)	21 (5)	C(2F)	5552 (10)	10489 (15)	7145 (6)	28 (2)
H(5)	318 (7)	987 (7)	889 (4)	29 (5)	C(3F)	6503 (14)	11375 (10)	6985 (7)	30 (14)
H(6)	104 (4)	937 (4)	887 (3)	5 (14)	C(4F)	7352 (12)	10994 (18)	6725 (7)	32 (17)
H(7)	316 (5)	1029 (6)	798 (3)	22 (5)	C(5F)	7268 (15)	9771 (18)	6609 (8)	36 (17)
H(8)	96 (9)	1057 (10)	857 (6)	38 (6)	C(6F)	6302 (14)	8918 (11)	6771 (7)	32 (14)
H(9)	188 (5)	957 (5)	924 (3)	17 (5)	H(11)	374 (5)	809 (5)	561 (3)	11 (9)
P(1)	2409 (2)	8716 (2)	6257 (1)	23 (2)	H(12)	254 (7)	745 (7)	517 (5)	25 (7)
P(2)	1500 (2)	6478 (2)	7024 (1)	23 (2)	H(21)	98 (7)	582 (7)	573 (4)	27 (6)
P(3)	4125 (2)	8055 (2)	7244 (1)	24 (2)	H(22)	159 (5)	501 (6)	614 (3)	4 (26)
C(1)	2916 (11)	7602 (10)	5663 (6)	24 (3)	H(31)	375 (7)	600 (8)	670 (4)	22 (8)
C(2)	1633 (10)	5778 (12)	6108 (6)	25 (4)	H(32)	458 (7)	672 (7)	631 (4)	26 (6)
C(3)	3854 (12)	6648 (11)	6502 (7)	25 (2)	H(51)	304 (8)	472 (8)	540 (5)	27[b]
C(4)	2844 (9)	6389 (9)	5894 (5)	23 (5)	H(52)	231 (8)	515 (8)	489 (5)	27[b]
C(5)	2977 (11)	5429 (11)	5249 (6)	27 (4)	H(53)	365 (7)	582 (7)	506 (5)	27[b]
C(1A)	3192 (8)	10248 (10)	6071 (6)	23 (4)	N(c)	1174 (11)	8039 (14)	778 (8)	35 (7)
C(2A)	3782 (10)	10425 (11)	5495 (6)	27 (5)	C(1c)[c]	1030 (29)	9213 (37)	813 (28)	61 (25)
C(3A)	4340 (10)	11608 (6)	5401 (7)	29 (10)	C(2c)	675 (25)	7458 (59)	1231 (19)	61 (40)
C(4A)	4356 (9)	12686 (11)	5880 (8)	28 (7)	C(3c)	2477 (26)	8244 (25)	917 (13)	49 (12)
C(5A)	3776 (11)	12522 (12)	6449 (6)	27 (5)	C(4c)	699 (37)	7312 (30)	13 (17)	56 (15)
C(6A)	3218 (8)	11322 (13)	6532 (5)	24 (3)	C(5c)	1555 (27)	10277 (31)	1496 (22)	48 (16)
C(1B)	994 (9)	8448 (8)	5710 (7)	24 (3)	C(6c)	836 (25)	6374 (30)	1491 (20)	47 (15)
C(2B)	879 (12)	8530 (9)	5005 (8)	27 (6)	C(7c)	3230 (37)	8437 (34)	368 (18)	49 (12)
C(3B)	−189 (19)	8360 (11)	4640 (6)	30 (10)	C(8c)	−541 (49)	7289 (66)	−170 (27)	55 (22)
C(4B)	−1156 (14)	8060 (12)	4936 (11)	30 (12)	H1(5c)	232 (14)	1034 (17)	166 (12)	48[b]
C(5B)	−1066 (13)	7975 (11)	5630 (11)	31 (8)	H2(5c)	109 (19)	1010 (22)	186 (14)	48
C(6B)	−3 (14)	8165 (9)	6031 (6)	26 (2)	H3(5c)	157 (17)	1105 (16)	140 (13)	48
C(1C)	−81 (9)	5888 (11)	6999 (6)	23 (4)	H1(6c)	156 (15)	632 (19)	140 (12)	47
C(2C)	−554 (12)	6542 (10)	7484 (6)	29 (7)	H2(6c)	23 (15)	561 (17)	124 (11)	47
C(3C)	−1738 (14)	6136 (14)	7501 (7)	31 (11)	H3(6c)	82 (17)	651 (19)	199 (10)	47
C(4C)	−2462 (10)	5049 (15)	7027 (9)	29 (9)	H1(7c)	336 (20)	925 (19)	29 (11)	49
C(5C)	−2030 (13)	4390 (11)	6534 (6)	29 (8)	H2(7c)	286 (25)	781 (23)	7 (11)	49
C(6C)	−839 (13)	4804 (13)	6521 (6)	27 (5)	H3(7c)	395 (19)	837 (21)	53 (11)	49
C(1D)	1809 (8)	5431 (11)	7548 (7)	22 (6)	H1(8c)	−78 (22)	701 (34)	−67 (11)	55
C(2D)	2254 (10)	5931 (9)	8260 (9)	26 (8)	H2(8c)	−55 (33)	811 (40)	−1 (19)	55
C(3D)	2492 (10)	5208 (18)	8696 (6)	31 (5)	H3(8c)	−105 (22)	673 (36)	6 (14)	55
C(4D)	2302 (12)	3971 (18)	8425 (10)	30 (6)	N,C(1S)[d]	3072 (16)	5386 (16)	691 (10)	32 (9)
C(5D)	1847 (14)	3429 (11)	7717 (11)	32 (10)	N,C(2S)	4571 (22)	6730 (23)	1647 (13)	43 (10)
C(6D)	1606 (11)	4186 (17)	7292 (6)	30 (7)	N,C(3S)	4946 (19)	6281 (22)	514 (11)	39 (10)
C(1E)	4884 (8)	7712 (12)	7983 (6)	25 (5)	N,C(4S)	4115 (24)	6072 (23)	922 (13)	37 (4)
C(2E)	4973 (10)	8405 (12)	8666 (9)	29 (6)					

[a] *U* is one-third the trace of the orthogonalized U_{ij} tensor, and the standard error is taken from Bessel's formula. [b] Set equal to the thermal parameter of the bonded C atom. [c] Atoms C(1c), C(2c), C(3c), and C(4c) are each bonded to N(c) and, respectively, to C(5c), C(6c), C(7c), and C(8c), forming the tetraethylammonium cation. [d] The four resolved atoms of the solvate molecule (S) have three-fourths occupancy.

anion and cation were assigned anisotropic temperature factors, with those for each hydrogen atom constrained equal to that of its bonded C atom.

All atoms in the final refinement cycles, except for the three H atoms in the disordered solvate molecule, were allowed to vary in position; however, the phenyl ring H atoms were constrained to be coplanar, each being 0.95 Å from its bonded C atom[11] and bisecting the C–C–C angle. The methyl-group H atoms at C(5) were also constrained at a distance of 0.95 Å, but the orientation of the rigid regular $C-CH_3$ tetrahedron was allowed to vary. Similarly, the H atoms in the four methyl groups of the cation were constrained at the same C–H distance in a regular tetrahedron of variable orientation, with the remaining two H atoms in each ethyl group forming a tetrahedron at the same C–H distance in a plane that is normal to and bisects the C–C–N angle with H–C–H = 109.4°. These 53 H atoms were assigned the same anisotropic temperature factor as their corresponding bonded C atom. The resulting final positional coordinates and RMS radial thermal displacements for the 74 unconstrained independent and 15 methyl-group H atoms are given in Table II. Final agreement indicators are $R(F_m) = 0.0226$, $R_w(F_m) = 0.0262$, and $S = 1.594$. The corresponding anisotropic thermal parameters are available as supplementary material.

The maximum shift/esd ratio in the final least-squares cycles was generally well under 2%; however, one parameter for each of the aliphatic H(51), H(52), and H(53) atoms had a ratio approaching 50%, while that for the hydridic H(1) and H(8) atoms approached 20%. Maximum and minimum features in the final difference map are less than ±0.45 e Å^{-3} and less than ±0.05 e Å^{-3} at Re(1) and Re(2). A view of the electron density in the plane of the disordered solvate molecule at 295 K is available as supplementary material. Most δR values on a normal probability plot,[12] on the basis of the X-ray diffraction F_m and F_c magnitudes, form a nearly linear array with zero intercept except for about 4% in the extrema that have a slightly larger slope. The overall slope $\mathcal{S}(\delta R) = 1.717$ indicates the average σF_m value has been underestimated by about 58%, but the linearity of the plot shows the measurements and model to be essentially free from systematic error.

The small crystal size available for neutron diffraction measurements resulted in a large ratio of weak- to strong-intensity reflections. Initial refinement of the atomic coordinates and thermal parameters of all atoms in Table II, except for those of the solvate molecule, was hence undertaken with the 1178 values of $F_m^2 > 4.5\sigma F_m^2$ by using another locally modified version of ORFLS.[10] The data were expanded at convergence to include first the 1687 values of $F_m^2 > 3\sigma F_m^2$ and finally the 2562 values of $F_m^2 > 1.5\sigma F_m^2$, in a successful test of the information content of the weaker reflections.

In the final neutron diffraction model, all atoms were unconstrained in position except for the three H atoms of the acetonitrile solvate, which were assumed to rotate freely, on the basis of a zero-order Bessel function,

(11) Churchill, M. R. *Inorg. Chem.* **1973**, *12*, 1213.

(12) Abrahams, S. C.; Keve, E. T. *Acta Crystallogr., Sect. A: Cryst. Phys., Diffr., Theor. Gen. Crystallogr.* **1971**, *A27*, 157.

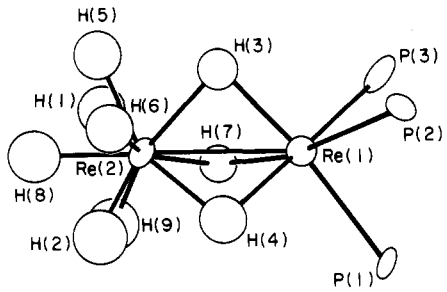

Figure 2. Arrangement at 80 K of H and P atoms around the Re(2)–Re(1) bond (see also Figure 1) with atom labeling and 50% probability thermal vibration ellipsoids. The right-handed rectangular coordinate axes for the Xα–SW calculation take the Re(1)–Re(2) bond center as origin with the z axis from Re(2) to Re(1) and the x axis from H(7) toward the origin (see text).

at a distance of 1.089 Å in a regular tetrahedral array about the methyl C atom. Anisotropic thermal parameters were assigned to all other atoms, except for those in the phenyl rings and H(1) to H(9), which were assigned isotropic values. The H atoms in the cation and H(11) to H(53) were given anisotropic thermal parameters identical with those of their bonded C atoms. The phenyl ring H atoms were similarly given isotropic thermal parameters identical with those of their bonded C atoms. Difference Fourier series showed that the solvate C and N atoms were ordered at 80 K. Also, two further H atoms were found within normal bonding distance of Re(2) in addition to those originally located by X-ray diffraction. Neutron scattering lengths used, in units of 10^{-12} cm, were $b_{Re} = 0.92$, $b_P = 0.513$, $b_C = 0.6648$, $b_N = 0.93$, and $b_H = -0.3741$.[13] Evidence for extinction was absent. The final model contained 558 variable parameters and resulted in $R(F_m) = 0.1336$, $R_w(F_m) = 0.0516$, and $S = 1.842$. The maximum final shift/esd ratio was 0.015 (for the phenyl H(2E)x coordinate). Analysis of the final δR normal probability plot[12] shows that both measurement and model are without major systematic error; the slope of the linear array is 1.39, with intercept −0.2. Maximum and minimum features in the final difference map are less than $\pm 0.15 \times 10^{-12}$ cm Å^{-3}. The final nuclear positional coordinates and RMS radial thermal displacements for the unconstrainted 126 atoms are given in Table III, with corresponding values of U_{ij} available as supplementary material.

Procedure for Molecular Orbital Calculations. SCF–Xα–SW calculations[14,15] for the C_s model complex $[Re_2(\mu\text{-}H)_3H_6(PH_3)_3]^-$ were carried out on a Cray-1 computer with a current version of the Xα–SW program package.[16] A right-handed rectangular coordinate system was taken with origin at the midpoint of, and z axis coincident with, the Re–Re bond (see also Figure 2). The xz plane is the mirror plane and contains atoms Re(1), Re(2), H(6), H(7), H(8), and P(2) with P(2) and H(6) at positive x coordinates. Coordinates in atomic units (1 bohr = 0.52917 Å) were derived from the bond distances and angles in the structure of $[Re_2(\mu\text{-}H_3)H_6(triphos)]^-$ and from the interatomic distances and angles in the PH_3 molecule.[17] Overlapping atomic sphere radii were taken as 89% of the atomic number radii.[18] These values gave a satisfactory virial ratio ($-2T/V = 1.000078$ for the nonrelativistic calculation). The outer sphere surrounding the molecule was centered at the valence electron weighted average of the atomic positions and was taken tangent to the outermost atomic spheres. A Watson sphere,[19] with a 1+ charge and the same radius and center as the outer sphere, was used to simulate the electrostatic interaction of the complex with its surrounding crystal lattice. Values of the α exchange-correlation parameter were as follows:[20,21] $\alpha_{Re} = 0.693\,25$, $\alpha_P = 0.726\,20$, and $\alpha_H = 0.777\,25$. In the extramolecular and intersphere regions α was taken as an average of the atomic sphere

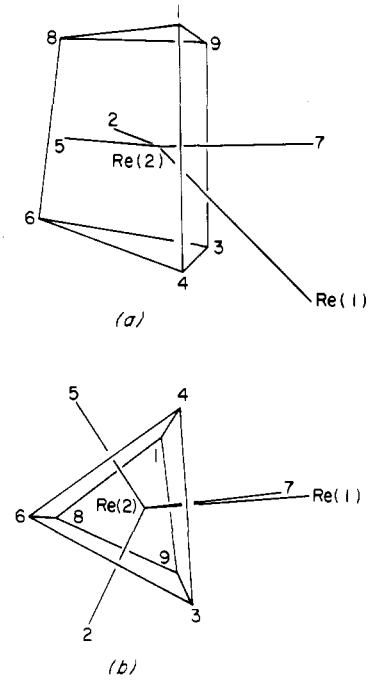

Figure 3. Distorted equatorially girded trigonal prismatic coordination of nine H atoms about Re(2), based on the structure at 80 K: (a) normal to prism trigonal axis, with Re(2)–Re(1) shown; (b) along prism trigonal axis, with Re(2)–Re(1) shown.

α values weighted by the number of valence electrons in the neutral atoms, giving $\alpha_{OUT} = \alpha_{INT} = 0.735\,94$.

The initial cluster potential for $[Re_2H_9(PH_3)_3]^-$ was constructed by superposing SCF–Xα charge densities for Re^0, P^0, and $H^{0.05556-}$. Partial waves through $l = 5$ in the extramolecular region, $l = 3$ in the rhenium spheres, $l = 2$ in the phosphorus spheres, and $l = 0$ in the hydrogen spheres were used to expand the wave functions. C_s symmetry was used to factor the secular matrix. The spin-restricted nonrelativistic ground-state calculations were carried through 53 iterations before relativistic effects[22] were included. An additional 35 iterations were required for convergence of the relativistic calculation to ±0.0001 Ry or better for the valence levels. A weighted average of the initial and final potentials for a given iteration was used as the starting potential for the next iteration; the proportion of final potential in the average was 10%. The final $[Re_2H_9(PH_3)_3]^-$ ground-state potential was used to search for virtual levels up to a maximum energy of −0.05 Ry and also served as the starting point for SCF calculations of Slater transition states for one-electron transitions to the virtual levels.[14,15] The transition-state calculations were carried out in spin-restricted form to give an estimate of the weighted average of the singlet and triplet transition energies.

Results and Discussion

Geometry of the Anion. The arrangement of H and P atoms about the Re(1)–Re(2) bond, illustrated in Figure 2, is of central interest. The bond lengths and angles given in Table IV show that P(1), P(2), P(3), H(3), H(4), and H(7) form a distorted octahedron about Re(1) with average Re(1)–P distance of 2.289 (4) [2.28 (3)] Å and Re(1)–H_{br} distance of 1.82 (6) [1.88 (3)] Å.[23] Atoms H(1) to H(9) form a distorted tricapped trigonal prism (14-deltahedron) about Re(2): at 80 K, H(3)–H(4)–H(6) and H(1)–H(8)–H(9) comprise the triangular faces of the prism while the equatorial H(2), H(5), and H(7) atoms each cap one of the quadrilateral faces (see Figure 3). At 295 K, an alternative orientation for the tricapped trigonal $Re(2)H_9$ prism appears probable, within the larger errors associated with the H atoms at room temperature (see below). The mean Re(2)–H_{ter} and Re(2)–H_{br} distances are respectively 1.65 (15) [1.66 (6)] and 1.81 (22) [1.83 (4)] Å. The Re(1)–Re(2) bond of distance 2.594 (1) [2.594 (14)] Å (this quoted esd has been arbitrarily increased from

(13) Koester, L.; Rauch, H.; Herkens, M.; Schröder, K. *Jahresber. Kernforschungsanlage Jülich* **1981**, 1755.
(14) Slater, J. C. *The Self-Consistent Field for Molecules and Solids: Quantum Theory of Molecules and Solids*; McGraw-Hill: New York, 1974; Vol. 4.
(15) Slater, J. C. *The Calculation of Molecular Orbitals*; Wiley: New York, 1979.
(16) Locally modified version of the revision by Mike Cook, Bruce Bursten, and George Stanly.
(17) Kuchitsu, K. *J. Mol. Spectrosc.* **1961**, *7*, 399. Sirvetz, M. M.; Weston, R. E. *J. Chem. Phys.* **1953**, *21*, 898.
(18) Norman, J. G., Jr. *Mol. Phys.* **1976**, *31*, 1191.
(19) Watson, R. E. *Phys. Rev.* **1958**, *111*, 1108.
(20) Schwarz, K. *Phys. Rev. B: Solid State* **1972**, *5*, 2466. Schwarz, K. *Theor. Chim. Acta* **1974**, *34*, 225.
(21) Slater, J. C. *Int. J. Quantum Chem., Symp.* **1973**, *No. 7*, 533.
(22) The program applies relativistic mass-velocity and Darwin corrections as described by: Wood, J. H.; Boring, A. M. *Phys. Rev. B: Condens. Matter* **1978**, *18*, 2701.
(23) Values in brackets, here and later in the text, refer to the neutron diffraction analysis: $\sigma(\langle d \rangle)$ is given by $[1/(n-1)\sum_{r=1}^{n}(d_r - \langle d \rangle)^2]^{1/2}$.

Table III. Final Nuclear Coordinates ($\times 10^4$) and Rms Thermal Displacements ($\times 10^2$ Å) at 80 K, by Neutron Diffraction

nucleus	*x*	*y*	*z*	U^a	nucleus	*x*	*y*	*z*	U^a
Re(1)	2454 (8)	8519(9)	7426 (5)	14 (3)	H(2A)	3742 (25)	9487 (29)	4980 (16)	21[b]
Re(2)	2107 (9)	10057 (9)	8549 (5)	15 (4)	H(3A)	4637 (25)	11545 (29)	4808 (17)	22
H(1)	3350 (31)	11038 (34)	9097 (18)	26 (7)	H(4A)	4773 (26)	13380 (32)	5723 (16)	22
H(2)	1012 (31)	10485 (35)	8388 (19)	27 (7)	H(5A)	3861 (23)	13262 (27)	6918 (15)	19
H(3)	1251 (26)	9176 (30)	7636 (16)	23 (8)	H(6A)	2819 (23)	11190 (26)	7048 (14)	19
H(4)	2400 (24)	8608 (27)	8445 (15)	20 (9)	H(2B)	1646 (23)	8805 (25)	4646 (14)	18
H(5)	2406 (27)	9802 (30)	9364 (16)	23 (8)	H(3B)	−220 (25)	8537 (29)	3943 (17)	22
H(6)	903 (27)	9213 (31)	8848 (17)	24 (8)	H(4B)	−1962 (27)	7993 (28)	4559 (16)	21
H(7)	3243 (24)	10167 (26)	7940 (14)	20 (8)	H(5B)	−1914 (25)	7657 (27)	5826 (15)	19
H(8)	1899 (31)	11104 (34)	9270 (20)	26 (7)	H(6B)	42 (23)	7953 (27)	6540 (15)	20
H(9)	2420 (31)	11378 (35)	8383 (20)	27 (7)	H(2C)	−83 (25)	7396 (30)	7790 (16)	21
P(1)	2342 (15)	8624 (16)	6205 (8)	13 (8)	H(3C)	−2134 (28)	6673 (33)	7880 (18)	24
P(2)	1476 (14)	6407 (15)	7027 (9)	11 (9)	H(4C)	−3307 (25)	4503 (27)	7069 (15)	20
P(3)	4006 (16)	7934 (17)	7255 (9)	17 (9)	H(5C)	−2535 (23)	3252 (28)	6209 (14)	19
C(1)	2863 (18)	7519 (16)	5565 (10)	19 (5)	H(6C)	−408 (22)	4080 (26)	6170 (14)	18
C(2)	1625 (14)	5645 (20)	6042 (8)	18 (4)	H(2D)	2196 (23)	6757 (30)	8518 (15)	19
C(3)	3873 (17)	6538 (15)	6427 (9)	17 (9)	H(3D)	2628 (25)	5583 (28)	9377 (17)	21
C(4)	2810 (11)	6267 (13)	5821 (7)	14 (4)	H(4D)	2393 (23)	3288 (27)	8832 (15)	19
C(5)	2951 (17)	5330 (18)	5165 (9)	20 (2)	H(5D)	1928 (26)	2452 (32)	7539 (16)	22
H(11)	3721 (30)	7958 (27)	5538 (15)	19[b]	H(6D)	1463 (23)	3670 (26)	6663 (15)	19
H(12)	2410 (25)	7241 (27)	5037 (19)	19	H(2E)	4255 (24)	8766 (27)	8811 (15)	19
H(21)	987 (26)	5794 (26)	5675 (15)	18	H(3E)	5321 (23)	8326 (26)	9901 (15)	19
H(22)	1499 (24)	4708 (36)	5970 (14)	18	H(4E)	6303 (24)	6801 (27)	9665 (15)	20
H(31)	3632 (24)	5690 (25)	6720 (14)	17	H(5E)	6338 (26)	5694 (29)	8333 (16)	21
H(32)	4530 (32)	6573 (24)	6241 (16)	17	H(6E)	5328 (25)	6170 (28)	7353 (17)	21
H(51)	3086 (24)	4542 (31)	5342 (15)	20	H(2F)	4611 (25)	10494 (27)	7355 (15)	20
H(52)	3705 (28)	5776 (28)	4922 (15)	20	H(3F)	6298 (26)	12229 (31)	7146 (16)	22
H(53)	2196 (27)	5028 (27)	4717 (16)	20	H(4F)	7953 (24)	11647 (26)	6693 (14)	19
C(1A)	3142 (12)	10147 (14)	6021 (8)	17 (6)	H(5F)	7981 (25)	9517 (27)	6531 (15)	20
C(2A)	3679 (14)	10251 (16)	5383 (9)	21 (4)	H(6F)	6293 (23)	7823 (27)	6770 (14)	19
C(3A)	4276 (15)	11426 (16)	5288 (9)	22 (4)	N(c)	1304 (9)	8288 (11)	845 (6)	19 (1)
C(4A)	4349 (15)	12566 (18)	5829 (9)	22 (4)	C(1c)	1086 (18)	9472 (16)	732 (10)	19 (7)
C(5A)	3806 (13)	12432 (15)	6452 (8)	19 (5)	C(2c)	644 (18)	7885 (18)	1469 (10)	17 (15)
C(6A)	3219 (13)	11271 (14)	6563 (8)	19 (5)	C(3c)	2581 (14)	8493 (23)	1112 (10)	21 (6)
C(1B)	975 (12)	8408 (14)	5675 (7)	17 (6)	C(4c)	914 (15)	7247 (20)	92 (10)	21 (5)
C(2B)	889 (13)	8560 (14)	4940 (8)	18 (5)	C(5c)	1622 (21)	10676 (21)	1398 (12)	24 (4)
C(3B)	−203 (14)	8412 (16)	4538 (9)	22 (4)	C(6c)	659 (20)	6610 (18)	1578 (12)	21 (7)
C(4B)	−1223 (15)	8085 (16)	4856 (9)	21 (4)	C(7c)	3365 (18)	8859 (22)	551 (12)	23 (3)
C(5B)	−1093 (13)	7961 (15)	5577 (8)	20 (5)	C(8c)	−389 (18)	6842 (24)	−167 (12)	24 (5)
C(6B)	−33 (13)	8094 (15)	5960 (9)	20 (5)	H1(1c)	178 (32)	9270 (28)	653 (15)	19[b]
C(1C)	−83 (12)	5792 (13)	6984 (7)	16 (7)	H2(1c)	1401 (26)	9639 (28)	252 (19)	19
C(2C)	−570 (14)	6490 (17)	7467 (9)	21 (4)	H1(2c)	−200 (31)	7840 (28)	1277 (16)	17
C(3C)	−1752 (16)	6051 (18)	7484 (10)	24 (4)	H2(2c)	1024 (28)	8479 (31)	1870 (18)	17
C(4C)	−2466 (14)	4865 (15)	7052 (8)	20 (4)	H1(3c)	2525 (25)	7729 (39)	1209 (16)	21
C(5C)	−1965 (13)	4144 (15)	6577 (8)	19 (5)	H2(3c)	2776 (23)	9233 (34)	1618 (18)	21
C(6C)	−797 (13)	4598 (14)	6528 (8)	18 (5)	H1(4c)	1127 (26)	6630 (36)	169 (17)	21
C(1D)	1833 (12)	5398 (13)	7573 (7)	16 (7)	H2(4c)	1312 (25)	7726 (29)	333 (17)	21
C(2D)	2138 (13)	5928 (17)	8356 (8)	19 (5)	H1(5c)	2537 (36)	10995 (32)	1477 (18)	24
C(3D)	2356 (14)	5155 (16)	8803 (9)	21 (4)	H2(5c)	1309 (29)	10507 (31)	1881 (22)	24
C(4D)	2299 (13)	3909 (15)	8520 (8)	20 (4)	H3(5c)	1286 (30)	11349 (37)	1252 (18)	24
C(5D)	2015 (15)	3390 (18)	7746 (9)	22 (4)	H1(6c)	1460 (34)	6646 (29)	1802 (18)	21
C(6D)	1725 (13)	4136 (15)	7279 (8)	20 (4)	H2(6c)	249 (28)	5809 (32)	1038 (20)	21
C(1E)	4752 (12)	7494 (14)	8002 (7)	17 (6)	H3(6c)	147 (30)	6363 (29)	1955 (19)	21
C(2E)	4742 (13)	8111 (16)	8746 (8)	19 (4)	H1(7c)	3270 (27)	9634 (35)	318 (18)	23
C(3E)	5357 (13)	7870 (15)	9341 (8)	19 (4)	H2(7c)	3210 (27)	8045 (33)	9 (20)	23
C(4E)	5901 (13)	6971 (15)	9207 (9)	20 (4)	H3(7c)	4201 (33)	9094 (30)	810 (18)	23
C(5E)	5883 (14)	6330 (16)	8469 (9)	21 (4)	H1(8c)	−553 (29)	6198 (34)	729 (21)	24
C(6E)	5339 (14)	6613 (16)	7865 (10)	21 (4)	H2(8c)	−698 (30)	7620 (37)	−218 (17)	24
C(1F)	5363 (12)	9105 (13)	7075 (7)	16 (7)	H3(8c)	−874 (32)	6335 (36)	145 (19)	24
C(2F)	5369 (14)	10345 (16)	7173 (8)	20 (4)	N(S)	2956 (13)	5690 (13)	750 (7)	23 (5)
C(3F)	6344 (15)	11275 (17)	7033 (9)	22 (5)	C1(S)	3937 (17)	6156 (19)	1007 (13)	25 (10)
C(4F)	7249 (13)	10960 (15)	6814 (8)	19 (5)	C2(S)	5104 (15)	6677 (18)	1358 (12)	24 (13)
C(5F)	7259 (14)	9730 (16)	6688 (9)	20 (4)	H(S)[c]				35 (2)
C(6F)	6285 (13)	8806 (16)	6823 (8)	19 (5)					

[a] See footnote *a* to Table II. [b] *U* values without parentheses indicate U_{ij} values of H atoms were constrained equal to those of the bonded C atom. [c] The three H atoms in the methyl group of the CH_3CN solvate were constrained to form a regular tetrahedron with C–H = 1.089 Å rotating freely about the C–C axis.

the least-squares value of the X-ray determination by the factor 1.67, but the neutron value is given as directly calculated by least squares) passes through the bridging H(3)–H(4)–H(7) face of the Re(1) octahedron and through the H(1)–H(4)–H(3)–H(9) face of the Re(2) prism (or H(3)–H(4)–H(7) face of the deltahedron); it makes an angle of 80.1 [87.6]° with the former plane and 32.7 [44.3]° with the latter face. Thus, Re(2) may be considered as capping one of the Re(1) octahedral faces while Re(1) caps an Re(2) deltahedron face, forming an Re(1)–Re(2)–H(7) angle of 46 (2) [45.5 (9)]° with the capping hydrogen. The Re atom and the nine H atoms bonded to Re(2) give it a coordination number of 10, an unprecedented value for a transition metal in a molecular compound, 9 being the largest value previously reported.

The bridging Re(1)–H and Re(2)–H distances are not significantly different; their average of 1.81 (13) [1.86 (4)] Å is close

Table IV. Bond Lengths (Å) and Angles (deg) in the $Re_2H_9P_3$ Grouping[a]

Re(1)–Re(2)	2.594 (1) [2.594 (14)]	Re(2)–H(1)	1.41 (9) [1.70 (4)]
–H(3)	1.79 (6) [1.90 (3)]	–H(2)	1.68 (9) [1.61 (4)]
–H(4)	1.77 (7) [1.89 (3)]	–H(3)	1.86 (6) [1.83 (3)]
–H(7)	1.89 (7) [1.85 (3)]	–H(4)	1.99 (7) [1.79 (3)]
–P(1)	2.287 (3) [2.30 (2)]	–H(5)	1.43 (9) [1.64 (3)]
–P(2)	2.286 (3) [2.29 (2)]	–H(6)	1.77 (5) [1.72 (3)]
–P(3)	2.292 (3) [2.25 (2)]	–H(7)	1.57 (7) [1.87 (3)]
		–H(8)	1.87 (12) [1.70((4)]
		–H(9)	1.71 (6) [1.56 (4)]
H(3)–H(6)	2.42 (8) [2.33 (4)]	H(3)–H(6)–H(4)	53 (2) [60 (1)]
H(3)–H(4)	2.18 (9) [2.32 (4)]	H(6)–H(4)–H(3)	62 (3) [60 (1)]
H(6)–H(4)	2.50 (8) [2.30 (4)]	H(4)–H(3)–H(6)	66 (3) [59 (1)]
H(1)–H(9)	2.33 (10) [1.88 (5)]	H(1)–H(9)–H(8)	60 (4) [60((2)]
H(9)–H(8)	2.37 (13) [1.88 (5)]	H(9)–H(8)–H(1)	59 (4) [60 (2)]
H(8)–H(1)	2.37 (14) [1.88 (5)]	H(8)–H(1)–H(9)	61 (4) [60 (2)]
H(2)–H(5)	3.06 (13) [2.81 (5)]	H(2)–H(5)–H(7)	52 (4) [64 (1)]
H(5)–H(7)	1.91 (11) [2.99 (4)]	H(7)–H(2)–H(5)	39 (3) [61 (1)]
H(7)–H(2)	2.42 (11) [3.06 (4)]	H(5)–H(7)–H(2)	89 (5) [55 (1)]
H(4)–H(1)	3.16 (11) [2.65 (5)]	H(3)–H(4)–H(1)	69 (3) [87 (1)]
H(6)–H(8)	1.66 (12) [2.09 (5)]	H(4)–H(1)–H(9)	46 (2) [87 (3)]
H(9)–H(3)	2.99 (9) [2.53 (5)]	H(1)–H(9)–H(3)	71 (3) [101 (2)]
		H(9)–H(3)–H(4)	49 (3) [83 (1)]
H(2)–H(3)	2.16 (11) [1.94 (5)]	H(3)–H(6)–H(8)	69 (5) [94 (2)]
–H(6)	2.44 (11) [1.83 (5)]	H(6)–H(8)–H(9)	26 (3) [97 (2)]
–H(8)	1.12 (12) [1.77 (5)]	H(8)–H(9)–H(3)	51 (3) [93 (2)]
–H(9)	2.91 (11) [1.74 (5)]	H(9)–H(3)–H(6)	21 (2) [76 (1)]
H(5)–H(1)	1.82 (11) [1.74 (5)]	H(6)–H(3)–H(1)	57 (2) [76 (1)]
–H(4)	1.70 (10) [1.95 (4)]	H(4)–H(1)–H(8)	77 (4) [89 (2)]
–H(6)	2.52 (10) [1.88 (4)]	H(1)–H(8)–H(6)	83 (5) [100 (2)]
–H(8)	3.17 (15) [1.83 (5)]	H(8)–H(6)–H(4)	112 (5) [94 (2)]
H(7)–H(1)	2.05 (10) [2.15 (4)]	Re(2)–H(3)–Re(1)	91 (3) [88 (1)]
–H(3)	2.12 (9) [2.35 (4)]	–H(4)–Re(1)	87 (3) [90 (1)]
–H(4)	2.28 (10) [2.23 (4)]	–H(7)–Re(1)	97 (3) [88 (1)]
–H(9)	3.12 (10) [2.05 (5)]		
Re(1)–Re(2)–H(1)	133 (3) [112 (1)]	P(1)–Re(1)–P(2)	88.0 (1) [88.9 (6)]
–Re(2)–H(2)	109 (3) [115 (1)]	–Re(1)–P(3)	86.0 (1) [86.7 (7)]
–Re(2)–H(5)	83 (3) [115 (1)]	P(2)–Re(1)–P(3)	85.0 (1) [84.0 (7)]
–Re(2)–H(6)	110 (2) [106 (1)]	P(1)–Re(1)–H(3)	98 (2) [95 (1)]
–Re(2)–H(8)	123 (4) [178 (1)]	–Re(1)–H(4)	172 (2) [171 (1)]
–Re(2)–H(9)	117 (2) [108 (1)]	–Re(1)–H(7)	106 (2) [103 (1)]
		P(2)–Re(1)–H(3)	99 (2) [102 (1)]
		–Re(1)–H(4)	88 (2) [95 (1)]
		–Re(1)–H(7)	164 (2) [168 (1)]
		P(3)–Re(1)–H(3)	174 (2) [174 (1)]
		–Re(1)–H(4)	101 (2) [102 (1)]
		–Re(1)–H(7)	104 (2) [97 (1)]

[a] See Figure 2 and also footnote *a* to Table I.

to the previously reported[24] (neutron diffraction) bridging Re–H distance of 1.878 (11) Å in $Re_2H_8(PEt_2Ph)_4$. The Re(1)–H_{br}–Re(2) bond angles do not differ significantly from 90°. The average Re–H terminal distance of 1.65 (15) [1.66 (6)] Å is in close agreement with the neutron values of 1.669 (18) Å in $Re_2H_8(PEt_2Ph)_4$,[24] 1.68 (1) Å in ReH_9^{2-},[25] and 1.688 (5) Å in $ReH_5(PCH_3(C_6H_5)_2)_3$.[26]

As shown in Figure 3, the H atom coordination polyhedron about Re(2) at 80 K forms a distorted equatorially tricapped trigonal prism. The expansion of one triangular face (H(3)–H(4)–H(6), mean edge length 2.37 (17) [2.32 (2)] Å) compared to the other (H(1)–H(8)–H(9), mean edge length 2.36 (2) [1.88 (1)] Å) is notable at 80 K as a consequence of the bridging character of atoms H(3) and H(4). Prism edge H(6)–H(8) at 1.66 (12) [2.09 (5)] Å is also shortened strongly compared to edges H(1)–H(4) and H(3)–H(9) (mean length 3.08 (12) [2.59 (8)] Å). These edge lengths may also be compared with those in the ReH_9^{2-} regular tricapped trigonal prism, where the triangular face edges are 2.08 (8) Å and the long edges of the rectangular faces are 2.37 (3) Å.[25] The edges of the triangle defined by the equatorial capping atoms, H(2), H(5), and H(7), with mean length 2.46 (58) [2.95 (13)] Å, are comparable to the corresponding 2.89 (13) Å in ReH_9^{2-}. Atoms H(2), H(5), and H(7) do not deviate greatly from coplanarity with Re(2); the largest deviation of an H atom from the best common plane is 0.029 (9) [–0.029 (3)] Å, while Re(2) is 0.003 [0.086] Å from this plane.

The distortions at 80 K in the tricapped trigonal prism may also be described in terms of the distances between equatorial and triangular face H atoms (see Figure 3a). Capping atoms H(2) and H(5) are equally close to the H(1)–H(8)–H(9) face at an average H–H distance of 1.77 (4) Å and to the H(3)–H(4)–H(6) face at an average distance of 1.90 (6) Å. By contrast, H(7) is 2.10 (7) Å from H(1)–H(8)–H(9) and 2.29 (8) Å from H(3)–H(4)–H(6). In the case of the ReH_9^{2-} ion, these twelve H–H distances are all equal at 1.90 (4) Å. It is noted that the H(7)–Re(2)–Re(1) plane is nearly normal (86.5°) to the mean H(1)–H(9)–H(3)–H(4) plane. In ReH_9^{2-}, the planes corresponding to H(1)–H(8)–H(9), H(2)–H(5)–H(7), and H(3)–H(4)–H(6) are parallel; with the present distortions, the equatorial plane is inclined at 11.3° to H(3)–H(4)–H(6) and at 5.4° to H(1)–H(8)–H(9), and face H(3)–H(4)–H(6) is inclined at 15.5° to H(1)–H(8)–H(9).

The orientation of, and corresponding distortions in, the tricapped trigonal Re(2)H_9 prism at 295 K may differ from that

(24) Bau, R.; Carroll, W. E.; Teller, R. G.; Koetzle, T. F. *J. Am. Chem. Soc.* **1977**, *99*, 3872.
(25) Abrahams, S. C.; Ginsberg, A. P.; Knox, K. *Inorg. Chem.* **1964**, *3*, 558.
(26) Emge, T. J.; Koetzle, T. F.; Bruno, J. W.; Caulton, K. G. *Inorg. Chem.* **1984**, 4012.

Table V. Principal Bond Lengths (Å) and Angles (deg) in the triphos–Re Grouping[a]

Re(1)–P(1)	2.287 (3) [2.299 (17)]	P(3)–C(3)	1.849 (12) [1.933 (24)]
–P(2)	2.286 (3) [2.288 (19)]	C(1)–C(4)	1.537 (14) [1.603 (22)]
–P(3)	2.292 (3) [2.253 (24)]	C(2)–C(4)	1.561 (14) [1.559 (20)]
P(1)–C(1A)	1.841 (11) [1.856 (21)]	C(3)–C(4)	1.547 (15) [1.570 (21)]
–C(1B)	1.865 (11) [1.812 (23)]	C(4)–C(5)	1.548 (15) [1.509 (21)]
–C(1)	1.850 (11) [1.856 (23)]	C(1)–H(11)	1.02 (7) [1.04 (5)]
P(2)–C(1C)	1.839 (11) [1.835 (21)]	–H(12)	0.99 (9) [1.03 (5)]
–C(1D)	1.843 (11) [1.829 (21)]	C(2)–H(21)	1.07 (9) [1.08 (5)]
–C(2)	1.834 (12) [1.908 (21)]	–H(22)	0.89 (6) [1.02 (6)]
P(3)–C(1E)	1.826 (12) [1.855 (23)]	C(3)–H(31)	0.89 (8) [1.19 (4)]
–C(1F)	1.871 (12) [1.918 (21)]	–H(32)	0.99 (9) [0.91 (6)]
Re(2)–Re(1)–P(1)	127.9 (1) [127.5 (7)]	Re(1)–P(3)–C(3)	115.1 (5) [118.5 (10)]
–Re(1)–P(2)	127.2 (1) [125.7 (6)]	P(1)–C(1)–C(4)	116.2 (8) [114.3 (12)]
–Re(1)–P(3)	128.4 (1) [129.8 (6)]	P(2)–C(2)–C(4)	114.6 (8) [113.4 (12)]
Re(1)–P(1)–C(1A)	117.8 (4) [117.1 (9)]	P(3)–C(3)–C(4)	115.2 (9) [111.7 (13)]
–P(1)–C(1B)	121.4 (5) [120.0 (9)]	C(1)–C(4)–C(2)	110.2 (10) [111.8 (14)]
–P(1)–C(1)	114.6 (4) [116.4 (11)]	–C(4)–C(3)	111.2 (11) [110.1 (12)]
–P(2)–C(1C)	119.4 (4) [120.9 (10)]	C(2)–C(4)–C(3)	112.0 (10) [115.1 (13)]
–P(2)–C(1D)	117.5 (5) [117.3 (9)]	H(11)–C(1)–H(12)	98 (7) [108 (2)]
–P(2)–C(2)	114.6 (4) [114.6 (10)]	H(21)–C(2)–H(22)	117 (7) [111 (2)]
–P(3)–C(1E)	118.7 (5) [121.1 (10)]	H(31)–C(3)–H(32)	103 (8) [109 (2)]
–P(3)–C(1F)	118.3 (5) [119.6 (11)]		
$(C_{ar}–C_{ar})_{max}$	1.401 (17) [1.449 (25)]	$(C_{ar}–H)_{max}$	[1.150 (46)]
$(C_{ar}–C_{ar})_{min}$	1.342 (18) [1.350 (23)]	$(C_{ar}–H)_{min}$	[0.919 (46)]
$(C_{ar}–C_{ar})_{av}$	1.374 (15) [1.408 (21)]	$(C_{ar}–H)_{av}$	[1.067 (53)]

[a] See footnote *a* to Table I.

Table VI. Selected Bond Lengths (Å) and Angles (deg) in the Tetraethylammonium Cation[a]

N(c)–C(1c)	1.42 (4) [1.527 (21)]	C(1c)–C(5c)	1.53 (6) [1.573 (25)]
–C(2c)	1.29 (3) [1.546 (18)]	C(2c)–C(6c)	1.51 (6) [1.536 (25)]
–C(3c)	1.54 (3) [1.553 (20)]	C(3c)–C(7c)	1.47 (5) [1.524 (35)]
–C(4c)	1.50 (3) [1.567 (20)]	C(4c)–C(8c)	1.54 (6) [1.544 (26)]
$(C_{aliph}–H)_{max}$	[1.178 (51)]		
$(C_{aliph}–H)_{min}$	[0.868 (62)]		
$(C_{aliph}–H)_{av}$	[1.049 (81)]		
C(1c)–N(c)–C(2c)	113.4 (35) [107.4 (13)]	C(2c)–N(c)–C(3c)	108.2 (22) [106.3 (12)]
–N(c)–C(3c)	110.0 (21) [113.7 (14)]	–N(c)–C(4c)	113.0 (30) [112.6 (13)]
–N(c)–C(4c)	104.1 (30) [109.4 (13)]	C(3c)–N(c)–C(4c)	108.0 (24) [107.5 (13)]

[a] See footnote *a* to Table I.

at 80 K. If the trigonal axis is taken as coincident with the Re(2)–Re(1) axis, then H(3)–H(4)–H(7) and H(8)–H(9)–H(1) comprise the triangular faces of the prism while equatorial H(2), H(5), and H(6) atoms each cap a quadrilateral face. The mean H–H distances in the triangular faces are 2.36 (2) and 2.19 (8) Å, respectively. The mean H–H distance is 2.67 (34) Å in the equatorial girdle. Prism face lengths of 2.05 (10) Å for H(1)–H(7), 2.39 (13) Å for H(8)–H(3), and 2.27 (9) Å for H(9)–H(4) are comparable in length with each other and with the corresponding lengths in the ReH_9^{2-} ion. The uncertainties in the H atom positions at 295 K, which may well exceed the esd's computed from the least-squares variance–covariance matrix, are such that further discussion of a change in the orientation of the Re(2)H_9 prism between 295 and 80 K is not at present warranted. A stereoview of the Re(2)H_9 atomic arrangement at 295 K is available as supplementary material. It may be noted that all hydridic H atoms in both $[Re_2H_9(triphos)]^-$ and ReH_9^{2-} are equivalent in solution.[1,25]

Analysis of the bonding in ReH_9^{2-}, based on SCF–Xα–SW calculations, has shown that there is a net H–H bonding interaction in that complex.[27] Although a similar analysis for $[Re_2H_9(PH_3)_3]^-$ has not been carried out, it is suggested that deformation of the ReH_9 coordination sphere in the dimer at 80 K may be explained by perturbation of the H–H bonding in ReH_9^{2-} through the coordination to $[Re(triphos)]^+$. We speculate as follows: the bridge bonding of atoms H(3) and H(4) drastically reduces their ability to engage in H–H bonding, both with each other and with atom H(6), leading to the expanding and tilting of triangular face H(3)–H(4)–H(6) and shortening of distance H(6)–H(8), with respect to the analogous face and distance in ReH_9^{2-}. Similarly, the bridge bonding of atom H(7) disengages it from equatorial–apical bonding with atoms H(1) and H(9), allowing these atoms to increase their bonding with each other and with atom H(8), leading to the contraction of triangular face H(1)–H(8)–H(9) as compared to the analogous face of ReH_9^{2-}.

The triply protonated Re–Re bond in the nonahydride dimer is very close in length to the triply H-bridged Re–Re bond distances reported in $Re_2H_4(PMe_2Ph)_4[P(OCH_2)_3CEt]_2$ of 2.597 (1) Å,[28] in $Re_2H_5(PMe_2Ph)_4[P(OCH_2)_3CEt]_2BF_4$ of 2.605 (2) Å,[28] in $[Re_2H_5(PPh_3)_4(CN\text{-}t\text{-}Bu)_2]PF_6$ of 2.604 (1) Å,[29] and in $Re_2H_6(PMe_2Ph)_5$ of 2.589 (1) Å.[30] The bond is significantly longer than the quadruply H-bridged bond in $Re_2H_8(PEt_2Ph)_4$ of 2.538 (4) Å.[24] Electron counting and assumption of the 18-electron rule predicts a Re–Re triple bond in $[Re_2H_9(triphos)]^-$, the other (μ-H)$_3$ complexes, and the (μ-H)$_4$ complex. Compared with non-hydrogen-bridged Re–Re bond lengths, the hydrogen-bridged distances are similar to that of an Re–Re double bond and are much longer than quadruple or triple bonds.[31]

(27) Ginsberg, A. P. In *Transition Metal Hydrides*; Bau, R., Ed.; Advances in Chemistry 167; American Chemical Society: Washington, DC, 1978; pp 201–214.

(28) Green, M. A.; Huffman, J. C.; Caulton, K. G. *J. Am. Chem. Soc.* **1982**, *104*, 2319.

(29) Allison, J. D.; Cotton, F. A.; Powell, G. L.; Walton, R. A. *Inorg. Chem.* **1984**, *23*, 159.

(30) Green, M. A.; Huffman, J. C.; Caulton, K. G. *J. Am. Chem. Soc.* **1981**, *103*, 695.

Table VII. Valence Molecular Orbitals of $[Re_2(\mu\text{-}H)_3H_6(PH_3)_3]^-$

level[a]	energy, eV	rel charge distribn, %[b]											basis functions[c]		intersphere charge	major bonding character
		Re(1)	Re(2)	2P(1)	P(2)	2H(1)	2H(2)	2H(3)	H(6)	H(7)	H(8)	Hp	Re(1)	Re(2)		
18a′	−0.858														74	
11a″	−0.867														75	
10a″	−1.042	29	52	9	0	0	5	2	0	0	0	2	d_{yz}	d_{yz}	35	Re–Re π^*_{yz}
17a′	−1.099	29	52	3	5	3	1	1	2	1	0	2	d_{xz}	d_{xz}	35	Re–Re π^*_{xz}
16a′	−1.167														78	
15a′	−4.071	82	0	10	1	0	0	0	0	0	0	6	$d_{x^2-y^2}$, d_{xz}		19	Re(1) nonbonding
9a″	−4.081	82	0	5	6	0	0	0	0	0	0	6	d_{xy}, d_{yz}		19	Re(1) nonbonding
14a′	−4.289	74	1	9	4	0	0	1	0	0	2	8	d_{z^2}		21	Re(1) nonbonding
8a″	−7.107	15	12	38	0	8	0	17	0	0	0	10	p_y, d_{xy}, d_{yz}	d_{yz}, d_{xy}, p_y	18	Re–P
13a′	−7.177	16	11	14	25	1	1	5	6	10	0	10	p_x, $d_{x^2-y^2}$, d_{xz}	d_{xz}, p_x, $d_{x^2-y^2}$	17	Re–P
12a′	−7.613	15	6	25	14	1	1	16	1	8	4	10	p_z, s		16	Re–P, Re–H_{br}
11a′	−8.592	17	30	4	10	1	9	1	19	3	2	4	d_{xz}, $d_{x^2-y^2}$	$d_{x^2-y^2}$	11	Re–H_{ter}
7a″	−8.663	21	25	17	0	25	0	6	0	0	0	5	d_{yz}, d_{xy}	d_{xy}	10	Re–H_{ter}
6a″	−8.980	0	0	29	16	0	0	0	0	0	0	55			0	P–H
5a″	−9.180	1	0	41	4	0	0	0	0	0	0	53			0	P–H
10a′	−9.192	1	0	20	25	0	0	0	0	0	0	53			0	P–H
9a′	−9.398	5	38	7	2	3	0	4	2	1	35	4		d_{z^2}	12	Re–H_{ter}
8a′	−9.605	2	38	1	1	29	20	2	4	3	1	1		$d_{x^2-y^2}$, d_{xy}, p_x	15	Re–H_{ter}
7a′	−9.759	2	1	30	15	0	0	1	0	0	1	50			6	P–H
4a″	−9.843	2	39	1	0	0	53	4	0	0	0	1		d_{xy}, d_{yz}, p_y	14	Re–H_{ter}
3a″	−9.939	1	0	21	25	0	0	0	0	0	0	52			4	P–H
6a′	−9.955	1	0	40	6	0	0	0	0	0	0	53			4	P–H
5a′	−10.236	19	24	11	5	7	6	11	6	4	1	6	s, d_{z^2}	d_{z^2}, p_z	12	σ Re–Re, Re–H_{br}
4a′	−10.630	14	35	1	3	4	0	8	11	23	0	1	d_{xz}, $d_{x^2-y^2}$	d_{xy}, $d_{x^2-y^2}$	10	π_{xz} Re–Re, Re–H_{br}
2a″	−10.735	11	38	3	0	17	2	27	0	0	0	1	d_{yz}, d_{xy}	d_{yz}, d_{xy}	9	π_{yz} Re–Re, Re–H_{br}
3a′	−13.307	4	29	1	0	16	16	10	7	4	12	1		s	18	Re–H_{ter}
1a″	−15.907	2	0	65	0	0	0	0	0	0	0	33			0	P–H
2a′	−15.912	2	0	22	43	0	0	0	0	0	0	33			0	P–H
1a′	−16.396	3	0	43	22	0	0	0	0	0	0	31			2	P–H

[a] The highest occupied level is 15a′. [b] Relative percentage of the total population of the level located within the indicated region. $\sum$(relative atomic sphere charges, over all atomic spheres) = 100%. The intersphere charge is shown in the last column of the table. The outer-sphere charge was small for all cases except virtual levels 11a″ (17.9%), 16a′ (17.1%), and 18a′ (18.0%). For levels in which the intersphere + outer-sphere charge is very large, the relative atomic sphere charge distribution is not given. 2P(1), 2H(1), 2H(2), 2H(3) each refer to the indicated sphere combined with its symmetry-equivalent sphere. Hp refers to the combined phosphine hydrogen spheres. [c] When more than 10% of the population of a level is located within the Re(1) or Re(2) spheres, the spherical harmonic basis functions contributing more than 10% of the charge in that region are listed in order of decreasing importance.

The triclinic symmetry imposes no geometrical constraints on any part of the $(C_2H_5)_4N^+[Re_2H_9(triphos)]^-\cdot CH_3CN$ complex; however, the triphos–Re(1) grouping closely approaches threefold symmetry, with Re(2)–Re(1)–C(4)–C(5) forming the pseudo-threefold axis. The maximum deviation of these four atoms from this axis is less than 0.05 (4) [0.12 (2)] Å, the C(4)–C(5) vector being inclined at 1.2 (5) [2.9 (7)]° to the Re(1)–Re(2) vector. Major distances and angles in this atomic grouping are given in Table V. The 16 atoms in the skeletal $Re_2P_3C_{11}$ group (i.e. all non-hydrogen atoms shown in Figure 1 except for those phenyl ring carbon atoms not bonded directly to phosphorus) deviate from threefold symmetry by less than 0.14 (12) [0.20 (11)] Å. The angles made by the normals to phenyl rings A, C, and E with the Re(2)–Re(1)–C(4)–C(5) axis are 87.8 [86.5], 85.8 [81.0], and 86.9 [88.7]°, respectively. The normals to rings B, D, and F however are inclined at 41.1 [38.9], 64.6 [70.2], and 55.8 [54.1]°.

The average Re–P = 2.288 (3) [2.28 (3)] Å distance in the nonahydride dimer may be compared with the average 2.271 (77) Å in $Re_2H_4(PMe_2Ph)_4[P(OCH_2)_3CEt]_2$,[28] 2.320 (17) Å in $ReH_5(PMe_2Ph)_3$,[30] 2.335 (2) Å in $Re_2H_8(PEt_2Ph)_4$,[24] 2.378 (16) Å in $[Re_2H_5(PPh_3)_4(CN\text{-}t\text{-}Bu)_2]PF_6$,[29] 2.381 (16) Å in $ReH_5(PMePh_2)_3$,[26] and 2.384 (30) Å in $ReH_5(PMe_2Ph)_3(C_5H_8)$.[32] The shortest reported value is 2.266 (3) Å in $Re_{12}P_{26}$.[33] The average Re–Re–P angle is 127.8 (6) [127.7 (21)]°. The average P–C distance of 1.846 (14) [1.867 (43)] Å is not significantly different from such values as the 1.840 (7) Å reported in $ReH_7(Ph_3P)_2$,[34] and 1.834 (10) Å in $[Re_2H_5(PPh_3)_4(CN\text{-}t\text{-}Bu)_2]PF_6$.[29] The aliphatic C–C average bond length of 1.548 (10) [1.56 (4)] Å and C–C–C bond angle of 111.1 (9) [112 (3)]° are both in the normal range.

The H atom positions associated with C(1), C(2), and C(3) (see Figure 1) were allowed to vary freely, as an internal check

(31) Cotton, F. A.; Walton, A. A. *Multiple Bonds Between Metal Atoms*; Wiley: New York, 1982. Some Re–Re distances are as follows: unbridged $\sigma^2\pi^4\delta^2$ bond in $Re_2Cl_6(PEt_3)_2$, 2.22 Å; unbridged $\sigma^2\pi^4\delta^2\delta^{*2}$ bond in $Re_2Cl_4(PEt_3)_4$, 2.22 Å; 1-Cl-bridged $\sigma^2\pi^2$ bond in Re_3Cl_4, 2.49 Å. The unbridged single-bond length in $(C_5H_5)_2Re_2(CO)_5$ is 2.96 Å.

(32) Green, M. A.; Huffman, J. C.; Caulton, K. G.; Rybak, W. K.; Ziolkowski, J. J. *J. Organomet. Chem.* **1981**, *218*, C39.

(33) Guérin, R.; Potel, M.; Sergent, M. *Mater. Res. Bull.* **1979**, *14*, 1335.

(34) Howard, J. A. K.; Mead, K. A.; Spencer, J. C. *Acta Crystallogr., Sect. C: Cryst. Struct. Commun.* **1983**, *C39*, 555.

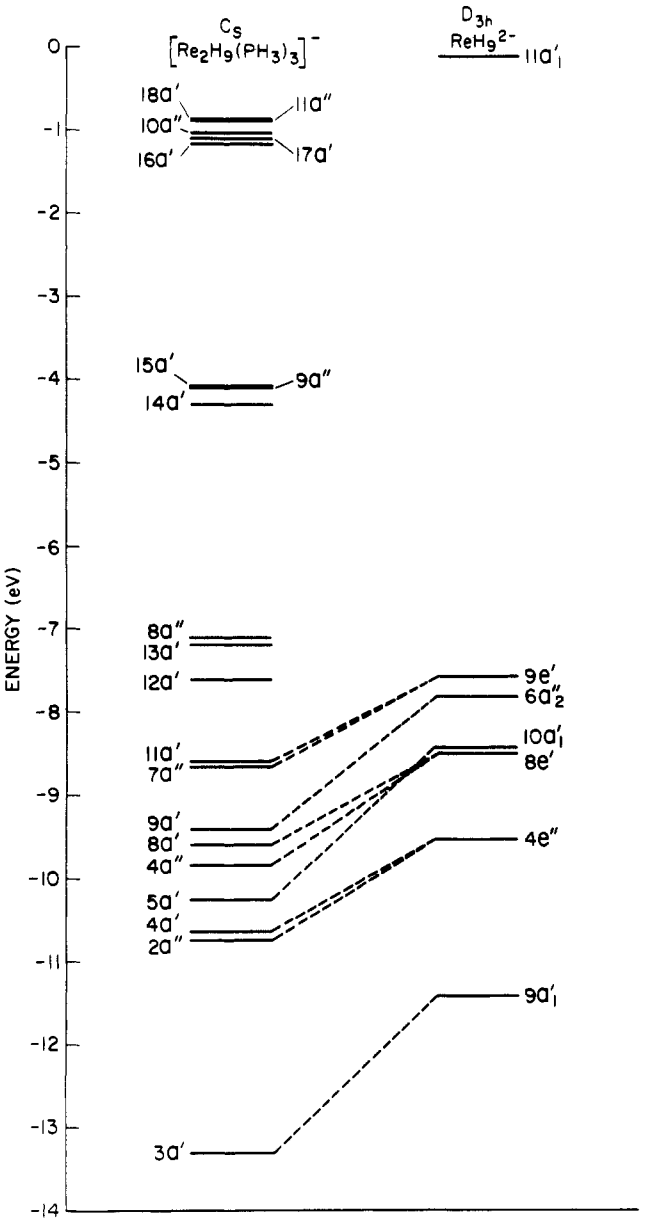

Figure 4. Valence energy levels for $[Re_2(\mu\text{-}H)_3H_6(PH_3)_3]^-$ and ReH_9^{2-} above −15 eV. Levels 15a′ and 9e′ are the HOMO's. The P–H bonding orbitals in PH_3 have been omitted from the diagram. The ReH_9^{2-} levels are from the nonrelativistic calculation in ref 27. The dashed lines correlate the ReH_9^{2-} orbitals with the $[Re_2H_9(PH_3)_3]^-$ orbitals to which they contribute; not all correlations are shown.

on the validity of the Re–hydrogen atom behavior, in the X-ray diffraction refinements. All H atom positions were varied in the neutron diffraction refinements. The average C–H distance of 0.98 (7) [1.05 (9)] Å (see Table V) is in excellent agreement with the average value of 1.073 Å for disubstituted paraffinic carbon.[35] The average H–C–H angle of 106 (10) [109 (2)]° is also normal.

Electronic Structure of $[Re_2(\mu\text{-}H)_3H_6(PH_3)_3]^-$. The calculated ground-state one-electron energies, charge distributions, and partial wave analyses for the valence molecular orbitals of $[Re_2H_9(PH_3)_3]^-$ are summarized in Table VII. Figure 4 is a diagram of the valence energy levels that also shows their correlation with the levels of ReH_9^{2-}.[27]

The occupied valence MO's of $[Re_2H_9(PH_3)_3]^-$ have energies in the range −4 to −16.4 eV. The three highest lying orbitals, 15a′ (the HOMO), 9a″, and 14a′, form a closely spaced group (−4.1 to −4.3 eV) that have most of their charge on the phosphine-coordinated Re atom: 15a′ and 9a″ may be described respectively as Re(1) $5d_{x^2-y^2}$, $5d_{xz}$ and Re(1) $5d_{xy}$, $5d_{yz}$ hybrid lone pairs, while 14a′ is mainly an Re(1) $5d_{z^2}$ lone pair. About 3 eV below these orbitals is a group of three levels, 8a″, 13a′, and 12a′, which comprise the Re–P bonding orbitals. Below the Re–P orbitals, in the energy range −8 to −13.3 eV, are the Re–H bonding orbitals. Three of these, 5a′, 4a′, and 2a″, are also Re–Re bonding, respectively σ, π_{xz}, and π_{yz}, giving rise to an Re–Re triple bond. The unusual situation of having the M–M π-bonding orbitals lower in energy than the σ-bonding orbital is explained by Figure 5, which shows the Re–H_{br} bonding interaction in the two M–M π orbitals to be much greater than in the σ orbital.

The correlation between ReH_9^{2-} and $[Re_2H_9(PH_3)_3]^-$ orbitals shown in Figure 4 helps in understanding the bonding in the dimeric complex. Of most interest is the parentage of the Re–Re and Re–H_{br} bonding orbitals. Figure 4 shows that the σ Re–Re orbital, 5a′, derives from ReH_9^{2-} orbital $10a_1'$, while the two π Re–Re orbitals, 4a′ and 2a″, derive from the doubly degenerate 4e″ orbital. In ReH_9^{2-}, Re–H bonding orbitals $10a_1'$ and 4e″ both have about 50% of their charge on the Re atom; this is by far the largest Re charge of any Re–H bonding orbital in ReH_9^{2-}.[27] The major Re spherical harmonic for $10a_1'$ is d_{z^2} while for 4e″ it is d_{xz}, d_{yz}.[27] Interaction of $10a_1'$ and the a′ and a″ components of 4e″ with vacant a′ and a″ orbitals on the ReP_3 fragment gives rise to the Re–Re triple bond as well as to Re–H bridge bonding.[36] It is the dual bonding character of these orbitals that allows the Re(2) atom to be 10-coordinated and accounts for the comparative weakness of the Re–Re triple bond, as indicated by its length compared to that of non-H-bridged Re–Re bonds.

Electronic Spectrum of $[Re_2(\mu\text{-}H)_3H_6(triphos)]^+$. Examination of Figure 4 and Table VIII indicates that the optical spectrum of $[Re_2H_9(PH_3)_3]^-$ should consist of a group of transitions in the visible region in the range ~3–3.5 eV (~350–400 nm), due to charge transfer from Re(1), followed by another group of transitions in the ultraviolet region in the range ~6–7 eV (~180–200 nm) due to charge transfer from phosphorus. The absorption spectrum of $[Re_2H_9(triphos)]^-$ (Table VIII), measured over the range 210–800 nm, is consistent with these expectations: a broad intense absorption with indistinct maxima at ~360 and ~335 nm is observed in the visible region, while in the ultraviolet region the extinction increases rapidly below 280 nm down to the lower limit of observation, with a shoulder appearing at 225 nm. The 225-nm shoulder coincides with an absorption found in free triphos.

Table VIII lists the energies, calculated by the spin-restricted transition-state method, for all transitions originating from the three highest lying occupied orbitals and terminating in one of the virtual orbitals given in Table VII. Also listed, where possible, are predicted intensities and the most important orbital components contributing to the intensity.[37] The calculated transition energies are in reasonably good agreement with the observed spectrum of the triphos complex. Major contributions to the absorption intensity are due to transitions from the nonbonding Re(1) d orbitals (15a′, 9a″, and 14a′) to the Re–Re π^*_{xz} and π^*_{yz} orbitals (17a′ and 10a″). Since the latter orbitals have their charge predominantly on Re(2), these transitions may be described as Re(1) → Re(2) charge transfer. The very weak feature observed at ~270 nm is probably a triplet component of one of the phosphine charge-transfer bands predicted below 210 nm.

Vibrational Spectrum of $[Re_2(\mu\text{-}H)_3H_6(triphos)]^+$. Infrared spectra of $Et_4N[Re_2H_9(triphos)]$ in Nujol mulls at ambient temperature show, in the terminal Re–H stretching region, a band at 1910 cm^{-1} with a broad shoulder extending from ~1950 to ~2100 cm^{-1} and a weak shoulder at ~1825 cm^{-1}. When the sample is cooled to liquid-nitrogen temperature, the spectrum in this region becomes much better resolved and the following seven absorptions may be clearly identified: 2080 (sh), 2030 (wm), 2000 (wm), 1975 (sh), 1942 (m), 1900 (ms), and ~1830 (sh) cm^{-1}. These are all presumably ν(ReH) frequencies, although the shoulders at 1975 and ~1830 cm^{-1} might be due to overtones of

(35) *Tables of Interatomic Distances and Configuration in Molecules and Ions*; Sutton, L. E., Ed. Chemical Society: London, 1965.

(36) Important Re–H_{br} bonding also occurs in the Re–P bonding orbital 12a′.

(37) Ginsberg, A. P.; O'Halloran, T. V.; Fanwick, P. E.; Hollis, L. S.; Lippard, S. J. *J. Am. Chem. Soc.* **1984**, *106*, 5430.

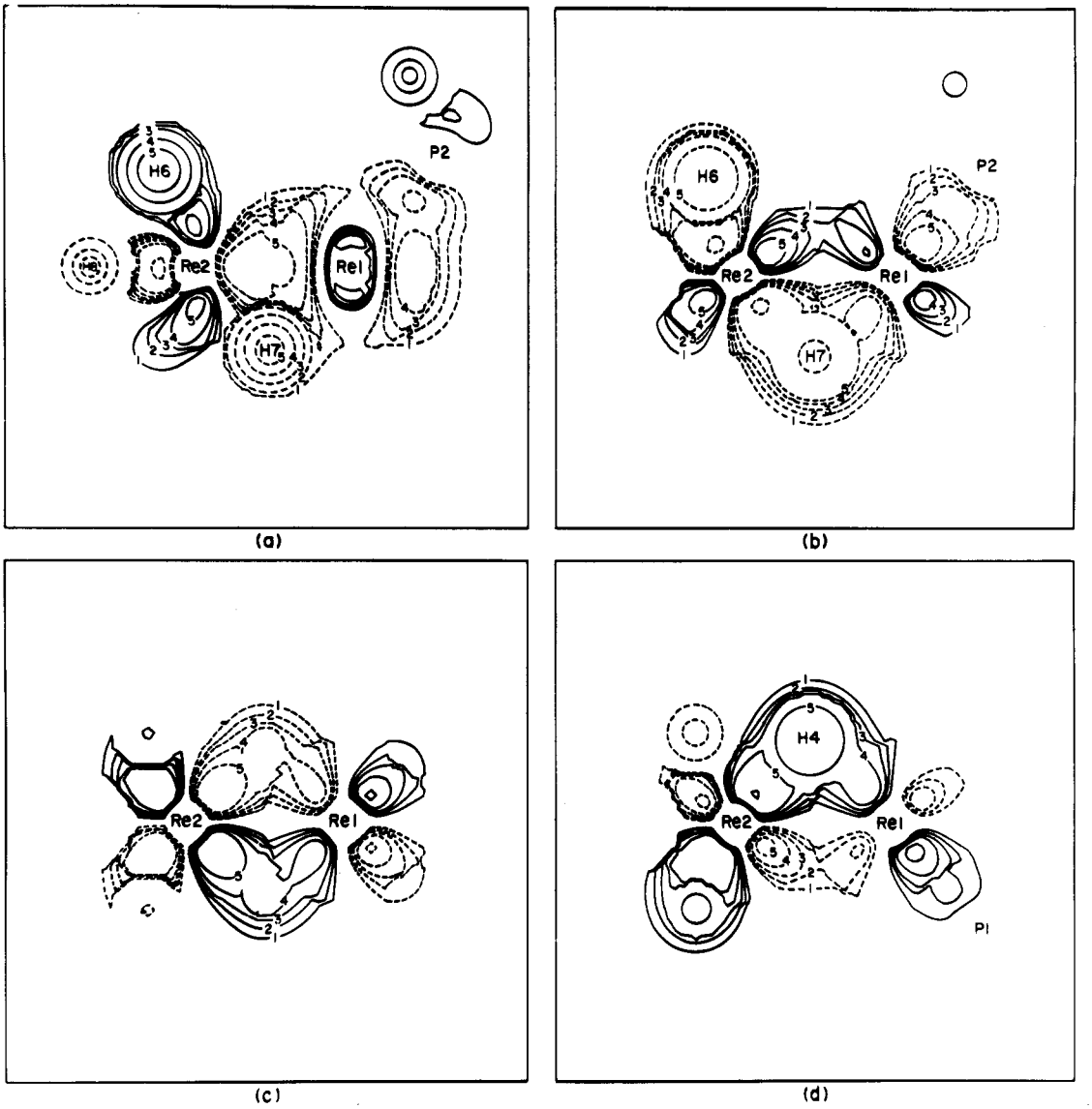

Figure 5. Wave function contour maps of the Re–Re and Re–H_{br} bonding orbitals in $[Re_2(\mu\text{-}H_3)H_6(PH_3)_3]^-$. Solid and broken lines denote contours of opposite sign having magnitudes indicated by the numerical labels 1, 2, 3, 4, 5, and 6, equal to 0.03, 0.04, 0.05, 0.065, 0.09, and 0.20 $(e/bohr^3)^{1/2}$, respectively: (a) level 5a′, the σRe–Re orbital in the *xz* plane; (b) level 4a′, the π_{xz} orbital in the *xz* plane; (c) level 2a″, the π_{yz} orbital in the *yz* plane; (d) level 2a″, the π_{yz} orbital in the plane through Re(1), Re(2), and H(4). Contours close to atomic centers are omitted for clarity.

Table VIII. Electronic Absorptions and Assignments for $[Re_2(\mu\text{-}H)_3H_6(triphos)]^-$

obsd values[a]			C_s,	calcd[b]	pred	
λ_{max}, nm	energy, eV	ϵ, M^{-1} cm^{-1}	transition	energy, eV	int[c]	descripn[d]
			9a″ → 17a′	3.33	m	Re(1) d_{xy}, d_{yz} → Re(2) d_{xz}
			15a′ → 17a′	3.33	s	Re(1) $d_{x^2-y^2}$, d_{xz} → Re(2) d_{xz}
~360	3.44	7.4×10^3	15a′ → 10a″	3.37	m	Re(1) $d_{x^2-y^2}$, d_{xz} → Re(2) d_{yz}
			9a″ → 10a″	3.38	s	Re(1) d_{yz} → Re(2) d_{yz}
			15a′ → 16a′	3.44		
			9a″ → 16a′	3.45		
			14a′ → 17a′	3.47	s	Re(1) d_{z^2} → Re(2) d_{yz}
~335	3.70	7.4×10^3	14a′ → 10a″	3.52	s	Re(1) d_{z^2} → Re(2) d_{xz}
			14a′ → 16a′	3.57		
			15a′ → 18a′	3.72		
			15a′ → 11a″	3.72		
			9a″ → 18a′	3.74		
			9a″ → 11a″	3.74		
			14a′ → 18a′	3.86		
			14a′ → 11a″	3.87		
~270 (sh)	4.59	vw				
225 (sh)	5.51	4.8×10^4				triphos absorption

[a] 1.14×10^{-4} M solution in acetonitrile measured in 1 and 10 mm path length cells. The ~360- and ~335-nm bands are strongly overlapped. [b] Spin-restricted transition-state calculations. [c] Qualitative intensity estimate as described in ref 37. [d] The most important components contributing to the transition intensity.

phenyl ring deformations. ν(ReH) frequencies for M_2ReH_9 salts have been reported in the range 1700–1950 cm^{-1} and show appreciable sensitivity to the nature of the cation.[38] Outside the terminal Re–H stretching region, the spectrum of $Et_4N[Re_2H_9$(triphos)] has two bands that are clearly due to neither Et_4N^+ nor the triphos ligand: a medium band at 958 cm^{-1} is assigned as ν(Re–H–Re) while a medium-strong band at 785 cm^{-1} could be either δ(Re–H) (cf. δ(Re–H) = 610–745 cm^{-1} for ReH_9^{2-} salts) or another ν(Re–H–Re) frequency.

Hydrogen Counting in $[Re_2H_9$(triphos)]$^-$. The initial formulation of $[Re_2H_9$(triphos)]$^-$ as $[Re_2H_7$(triphos)]$^-$ was based on a ^1H NMR counting experiment that gave H/Re_2 = 7.1 from integration of the τ 15.62 high-field singlet with respect to the eight hydrogens of the $-CH_2N$ quartet.[1] This result was supported by the X-ray structure determination, which clearly located and refined seven Re-bonded H atoms in a rational structure.[1] Subsequent to definitively establishing, by neutron diffraction analysis, that two additional hydrogen atoms are present, we repeated the NMR counting experiment on a machine with an improved computer-controlled integration system. The values obtained for H/Re_2, with the reference peak for the integration in parentheses, are as follows: 8.85 (τ 2.25, ortho Ph H, 12); 8.59 (τ 3.10, all other Ph H, 18); 8.23 (τ 6.70, CH_3CH_2N quartet, 8); 8.75 (τ 7.70, CH_3CN, 3); 8.15 (CH_3CH_2N + CH_3C of triphos, 15); mean H/Re_2 8.5 ± 0.3. Since H/Re_2 must be odd to give a diamagnetic molecule, this result is consistent with the correct stoichiometry. As discussed above, more extensive analysis of the X-ray scattering data finally revealed the two additional H atoms, although their contribution is significantly less than that of the seven H atoms originally located. We conclude from all this that counting H atoms in hydride complexes, especially rhenium–H_9 systems, is as difficult today as it was 20 years ago![25]

Tetraethylammonium Cation. The accuracy with which the atomic positions in the cation have been determined at 295 K is rather low due to the large and strongly anisotropic cationic amplitudes of vibration (see the supplementary material) but is as expected for the ion at 80 K. The average N–C distance (see Table VI) of 1.44 (11) [1.548 (17)] Å and the C–C distance of 1.51 (3) [1.544 (21)] Å do not however differ significantly from the standard values of 1.479 and 1.537 Å, respectively.[35] All bond angles are also normal.

Solvate Acetonitrile and Phase Transition. It was realized at an early stage in the X-ray refinement that the solvate molecule was disordered at 295 K, with the C and N atoms lying in a well-defined plane (see the supplementary material). The acetonitrile molecule at 295 K may be described as occupying (over all unit cells) at least three positions, with one atom at the apices of an equilateral triangle (length of side about 2.39 (5) Å) and one near the center of the triangle. Each atom undergoes strongly anisotropic motion, with mean amplitude greater than 0.3 Å. With approximately equal maximum electron densities (~3.5–5 e $Å^{-3}$) at the four resolved atomic peaks (see Figure 6 in the supplementary material), it is likely that the CH_3CN atomic motion is substantially greater at one end (presumably N) than the other. The resulting large amplitudes would account for the unresolved atomic peaks. The C and N atoms in the solvate molecule are completely ordered at 80 K (see Table III), with the methyl group H atoms rotating freely. It is to be noted that the *c* axis decreases in length by 0.696 Å, on cooling from 295 to 80 K, corresponding to an expansion coefficient of 170 × 10^{-6} K^{-1}; the *a*- and *b*-axis coefficients are normal, at 15 × 10^{-6} and 12 × 10^{-6} K^{-1}, respectively. The major change in the *c* axis is directly associated with the order–disorder transition, as illustrated by the stereoviews of the content of a unit cell at 295 and 80 K (see below). The normal to the solvate disorder plane at 295 K is inclined at 71° to the *c* axis, with a major molecular axial component inclined at 32°. Below the phase transition, the molecular axis is oriented at an angle of 75° to the *c* axis. The resulting 43° angular rotation at the phase transition of the one-third solvate molecule present in the orientation closest to the *c* axis is expected to produce a contraction in length of about 1 Å, consistent with observation. An entropy change at the ordering temperature was not detected calorimetrically, presumably due to the solvate representing only 3.5% of the total molecular mass.

Crystal Packing. A stereoview of the content of one unit cell at both 295 and 80 K is available as supplementary material. The solvate may be seen therein to be approximately midway between cation and anion and normal to the closest contact directions. Most intermolecular contacts at either temperature are about 3.5 Å, with hydrogen atoms excluded, but that between N, C(S) and a C atom in ring E is only 3.30 (3) Å at both temperatures. No contact between the cation and other atoms is less than 3.5 Å.

Comparison of X-ray and Neutron Results. The X-ray results measured at 295 K together with the neutron results at 80 K allow a detailed analysis to be made of the conformational changes that occur within the anion over this temperature range, although this is not presented here. In addition, the two studies provide complementary connectivity information. The interatomic distances and angles given by the X-ray study are highly reliable throughout the anion, although with somewhat reduced accuracy for the H atoms; those in the cation and solvate molecule are lessened by the large thermal motion at room temperature. The precision of the neutron results is limited by the small crystal size but nevertheless provides very reliable H atom positions. The combined results from the two determinations hence describe the anion complex with greater reliability than those of either taken separately.

Acknowledgment. Research at Brookhaven National Laboratory was performed under Contract DE-AC02-76CH00016 with the U.S. Department of Energy and supported by its Division of Chemical Sciences, Office of Basic Energy Sciences. It is a pleasure to thank Fred Schilling for measuring the NMR spectra, J. L. Bernstein and L. E. Zyontz for their preliminary X-ray measurements and assistance in obtaining an initial partial structural model, K. Nassau for his calorimetric measurements, J. Henriques for technical assistance during the neutron diffraction experiment, and R. K. McMullan for helpful discussion.

Registry No. $Et_4N^+[Re_2(\mu\text{-}H)_3H_6$(triphos)]$^-\cdot CH_3CN$, 102286-20-4.

Supplementary Material Available: Tables of final coordinates for all constrained atoms at 295 K and the final U_{ij} anisotropic temperature coefficients at 295 and 80 K, figures of the electron density in the plane of the disordered solvate molecule at 295 K and the nuclear density in a quadrilateral face of the $Re(2)H_9$ trigonal tricapped prism, and stereoviews of the content of one unit cell both at 295 and at 80 K (10 pages). Ordering information is given on any current masthead page.

(38) Ginsberg, A. P.; Sprinkle, C. R. *Inorg. Chem.* **1969**, *8*, 2212.
(39) McMullan, R. K.; Andrews, L. C.; Koetzle, T. F.; Reidinger, F.; Thomas, R.; Williams, G. J. B., unpublished work.